Understanding Sterol–Membrane Interactions Part I: Hartree–Fock versus DFT Calculations of ^{13}C and ^{1}H NMR Isotropic Chemical Shifts of Sterols in Solution and Analysis of Hydrogen-Bonding Effects

Franck Jolibois,[b] Olivier Soubias,[a] Valérie Réat,[a] and Alain Milon*[a]

Abstract: ^{1}H and ^{13}C NMR chemical shifts are exquisitely sensitive probes of the local environment of the corresponding nuclei. Ultimately, direct determination of the chemical shifts of sterols in their membrane environment has the potential to reveal their molecular interactions and dynamics, in particular concerning the hydrogen-bonding partners of their OH groups. However, this strategy requires an accurate and efficient means to quantify the influence of the various interactions on chemical shielding. Herein the validity of Hartree–Fock and DFT calculations of the ^{13}C and ^{1}H NMR chemical shifts of cholesterol and ergosterol are compared with one another and with experimental chemical shifts measured in solution at 500 MHz. A computational strategy (definition of basis set, simpler molecular models for the sterols themselves and their molecular complexes) is proposed and compared with experimental data in solution. It is shown in particular that the effects of hydrogen bonding with various functional groups (water as a hydrogen-bond donor and acceptor, acetone) on NMR chemical shifts in $CDCl_3$ solution can be accurately reproduced with this computational approach.

Keywords: ab initio calculations · density functional calculations · hydrogen bonds · NMR spectroscopy · steroids

Introduction

Cholesterol is an essential component of cellular plasma membranes in higher organisms. It interacts with membrane phospholipids and influences their physicochemical properties. The important membrane properties that are directly or indirectly influenced by membrane levels of cholesterol include solute permeability in bilayer membranes,[1] phospholipid acyl chain mobility and orientational order in bilayer membranes,[1–3] and lateral packing density of phospholipids in monolayer membranes.[4,5] Cholesterol also has a marked influence on lateral phase separations,[6] and on the effective free volume of membranes,[7] two parameters which are directly related to the flexibility of membrane proteins (e.g., ion channels, enzymes) and hence to their function in membranes (for recent reviews on physical studies of cholesterol–phospholipid interactions, see McMullen and McElhaney[8] and Ohvo-Rekilä et al.[9]). Besides affecting properties of the host membrane, cholesterol itself is subject to restrictions on its motion. In fact, the lipid bilayer provides a highly anisotropic medium that determines the preferred location of cholesterol and governs the extent of motional fluctuations of thermally excited cholesterol.[10,11]

In a membrane bilayer cholesterol inserts normal to the plane of the bilayer, with its hydroxy group in close vicinity to the ester carbonyl group of glycerophospholipids and the amide bond of sphingolipids, and its alkyl side chain extending towards the center of the bilayer.[12–16] The largest contribution to cholesterol–phospholipid interactions appears to be from van der Waals forces and hydrophobic forces.[17,18] Furthermore, it has been suggested that the interactions of cholesterol with sphingolipids and glycerophospholipids can further be strengthened by hydrogen bonding of the cholesterol hydroxy group to the polar head group and interfacial regions in the lipids.[8,19,20] There have been many suggestions of hydrogen bonding between cholesterol and certain atoms of phosphatidylcholine,[12,21–27] but so far there are limited direct experimental data supporting these proposals.[12,28]

To analyze the interactions between membrane lipids and cholesterol, it is necessary to perform data acquisition directly on the membrane–cholesterol system. Among the dif-

[a] Dr. O. Soubias, Dr. V. Réat, Prof. Dr. A. Milon
Institut de Pharmacologie et de Biologie Structurale
CNRS and University P. Sabatier
205 rte de Narbonne, Toulouse (France)
Fax: (+33) 561-175-424
E-mail: alain.milon@ipbs.fr

[b] Dr. F. Jolibois
Laboratoire de Physique Quantique, UMR 5626, IRSAMC
University P. Sabatier
118 rte de Narbonne, Toulouse (France)

Supporting information for this article is available on the WWW under http://www.chemeurj.org/ or from the author: Selected computational and experimental data.

DOI: 10.1002/chem.200400245

ferent experimental methods available to study sterol–membrane molecular systems, solid-state NMR spectroscopy is a powerful tool that allows the investigation of amorphous and partly mobile biological entities directly in the liquid-crystalline lipid bilayers. Comparing the isotropic chemical shift δ of cholesterol in its membrane environment with those obtained in organic solvents such as CCl_4 or $CHCl_3$ would potentially reveal the nature of lipid–cholesterol interactions. Unfortunately, it remains almost impossible to extract specific microscopic information directly from these experimental values, and the help of theoretical models is necessary to perform this particular task.

Recent developments and implementations in quantum chemistry allow nowadays the accurate treatment of theoretical chemical shielding.[29–32] Theoretical investigation of sterol-type molecules is a task that can be accomplished with standard quantum-chemical methods.[33,34] Geometry optimization, determination of theoretical spectroscopic data such as NMR chemical shift and analysis of intermolecular interactions can be treated with a good level of accuracy for this kind of medium-sized molecular systems. Thus, combining quantum-chemical treatment and NMR experiments should result in a better interpretation of experimental isotropic chemical shifts δ_{iso}. Clearly, the complete quantum mechanical treatment of cholesterol–membrane system is unachievable. However, one can approach the simulation of these kinds of complexes by choosing adequate molecular models. Before this, it is necessary to calibrate a method that permits an accurate theoretical treatment with a low computational cost.

The first part of the present work concerns the determination of a computational strategy that allows the calculation of theoretical isotropic chemical shifts of sterols. To this end, we performed two types of calculations using either Hartree–Fock (HF) or hybrid DFT (B3LYP)[35,36] with medium-size basis sets on single cholesterol and ergosterol molecules. The conclusion that emerged is that HF is sufficient to reproduce the ^1H and ^{13}C isotropic NMR spectra of these two molecules in chloroform solution with good accuracy and with a small computational effort. This first study revealed a conformational property that is necessary to reproduce liquid-phase NMR spectra of cholesterol and ergosterol. The 3β-OH hydroxy hydrogen atom (see Scheme 1 for atom numbering) can adopt three rotational conformations (i.e., *gauche*(+), *gauche*(−), and *anti*) that are almost isoenergetic (within 1 kcal mol^{-1}). These three conformations exhibit different theoretical NMR spectra, especially for C2 to C4 and the hydrogen atoms to which they are connected. We show that each rotamer taken separately cannot reproduce the experimental NMR spectrum and that one must take into account the average value of isotropic chemical shifts to reproduce ^1H and ^{13}C NMR spectra of sterols in chloroform solution.

The second part of this work is related to the influence of different hydrogen-bonding partners on chemical shifts of cholesterol. Experimental ^{13}C chemical shift variations were obtained by titration of cholesterol with acetone and water in chloroform solution. Comparison of δ_{iso} obtained for such samples with chemical shifts of pure cholesterol demonstrated that the differences are mainly located on rings A and B (C1–C6). These experimental variations have been simulated by means of theoretical models involving simple interactions between one acetone (or water) molecule and the hydroxy group of cholesterol. An HF quantum-chemical calculation revealed its ability to correctly reproduce experimental ^{13}C chemical shift variations. From this theoretical investigation, we have also extracted information about the specific influence of hydrogen bonds on NMR spectra. We were able to separate two types of interaction—either with the hydrogen or the oxygen atom of the hydroxy sterol group—that result in inverse modifications of ^{13}C NMR spectra.

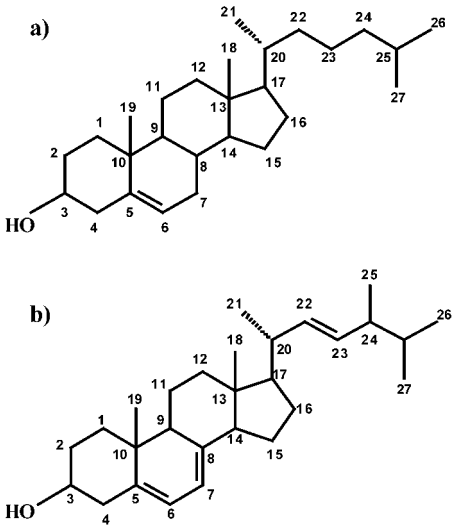

Scheme 1. Carbon atom numbering of cholesterol (a) and ergosterol (b). Rings A and B are defined by atoms 1 to 10.

Results and Discussion

Chemical shifts of pure cholesterol and ergosterol: The geometry of the cholesterol molecule was optimized according to the two different computational schemes described in the Experimental Section. The starting geometry for HF geometry optimization was the crystal structure,[37] from which side chain atoms C23–C27 were deleted, with a *gauche*(−) conformation for the hydroxy hydrogen atom (C2-C3-O-H ≈ −60°; see Scheme 1 for atom numbering and Figure 1 for definition of angle).

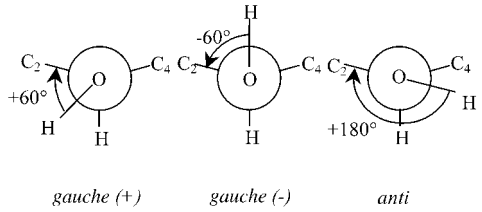

Figure 1. Newman representation of the three rotational isomers around the C3−O bond. These isomers are discriminated according to C2-C3-O-H dihedral angle.

The HF-optimized geometry was used as the starting point for the DFT optimization. As is well known, DFT and HF structures are not identical, but we will not discuss this point in the present article. We focus our attention on the quality of NMR isotropic chemical shifts calculated with our different computational schemes in comparison with experimental data (our work and ref. [38]). To evaluate the aptitude of each strategy for reproducing liquid isotropic chemical shifts of pure cholesterol, Pearson correlation coefficients R of the least-squares regression line (theory versus experiment) were calculated. One observes that DFT ($R=0.9993$) gives a better fit to experiment than HF ($R=0.9980$) when ^{13}C isotropic chemical shifts are considered (Table 1).

Table 1. Cholesterol ^{13}C and ^{1}H theoretical chemical shift variations compared with experiment, $\delta_{theo}-\delta_{exptl}$ (in ppm), calculated for atoms in positions 2–4.[a]

Position	Hartree–Fock							
	gauche(+)		*gauche*(−)		*anti*		Mean	
	^{13}C	^{1}H	^{13}C	^{1}H	^{13}C	^{1}H	^{13}C	^{1}H
2 (a)	1.37	0.29	1.31	−0.28	−1.44	0.27	0.42	0.09
2 (e)		−0.37		0.21		0.17		0.01
3	−3.13	0.07	−3.03	0.20	−3.10	0.07	−3.09	0.11
4 (a)	−2.37	0.10	0.38	−0.42	0.60	0.15	−0.46	−0.06
4 (e)		0.16		0.21		−0.38		0.00
R	0.9979	0.9887	0.9980	0.9869	0.9980	0.9882	0.9981	0.9936
Position	Density functional theory							
	gauche(+)		*gauche*(−)		*anti*		Mean	
	^{13}C	^{1}H	^{13}C	^{1}H	^{13}C	^{1}H	^{13}C	^{1}H
2 (a)	3.37	0.11	3.31	−0.36	−0.41	0.08	2.09	−0.05
2 (e)		−0.47		0.02		−0.05		−0.17
3	−0.25	0.17	−0.14	−0.01	−0.14	0.16	−0.18	0.11
4 (a)	−0.32	0.09	3.56	−0.33	3.85	0.15	2.36	−0.03
4 (e)		−0.12		−0.03		−0.53		−0.23
R	0.9992	0.9834	0.9993	0.9832	0.9990	0.9823	0.9994	0.9873

[a] Chemical shifts were calculated by HF and DFT strategies (see text for details) for the three rotamers of cholesterol. The Pearson correlation coefficient R of the least-squares regression line (theory versus experiment) was calculated for all carbon or hydrogen atoms. Experimental chemical shifts were determined in chloroform solution as indicated in the Experimental Section. Better R values are obtained by using mean values, both in the case of ^{13}C and ^{1}H. (a) and (e) denote axial and equatorial protons, respectively.

On the other hand, the HF strategy is slightly better than DFT for ^{1}H isotropic chemical shifts, with $R(HF)=0.9869$ and $R(DFT)=0.9832$. However, while R values shows that the average description of NMR spectrum is theoretically appropriate, several important differences between theory and experiment can be noted if one examines the details of ^{13}C and ^{1}H isotropic chemical shifts of the *gauche*(−) conformation (see Table 1). These differences essentially concern the region of cholesterol that is close to the hydroxy group [C2, C3, C4, H2, H3, and H4]. More specifically, the chemical shift calculated for axial hydrogen attached to C2 and C4 is too small compared with experimental values. The theoretical chemical shift of equatorial H2 and H4 is too large with the HF calculation and almost identical to the experimental value with the DFT method. This can be interpreted in term of interactions between hydrogen atoms. For the *gauche*(−) conformation, the hydroxy hydrogen atom adopts an axial type of configuration. Consequently, axial hydrogen atoms attached to C2 and C4 exhibit a more pronounced shielding due to interaction with the electronic density of the hydroxy hydrogen atom. On the other hand, equatorial hydrogen atoms attached to these two carbon atoms do not interact directly with the hydroxy hydrogen atom and are more deshielded. Considering that the main effect is due to the orientation of the hydroxy hydrogen atom, one can assume that other orientations might induce different chemical shifts. Consequently, two other rotamers, *gauche*(+) (C2-C3-O-H ca. +60°) and *anti* (C2-C3-O-H ca. 180°) were optimized. The structures of these three isomers are almost isoenergetic (maximum energy difference ca. 1 kcal mol^{-1} at the HF or DFT level). In the case of the *gauche*(+) conformation, the major effect is observed for the hydrogen atom attached to C2, and especially for the equatorial hydrogen atom that exhibits a large shielding compared with experimental value (difference of 0.4–0.5 ppm). On the other hand, for the *anti* conformation, the main difference compared with the experimental value is observed for the equatorial hydrogen atom H4(e) attached to C4 (difference of 0.4–0.5 ppm). In both cases, the interaction of the hydroxy hydrogen atom is essentially localized in the vicinity of the equatorial hydrogen atom (H2 for *gauche*(+) and H4 for *anti*), which induces a large shielding compared with experiment. Consequently, none of these structures is able to correctly reproduce isotropic NMR chemical shifts obtained in solution. Nevertheless, one must not forget that NMR experiments are generally performed at room temperature and thus observed chemical shifts correspond to average values over many conformations. Accordingly, we calculated ^{1}H and ^{13}C isotropic chemical shifts as average values over the three rotamers. First, by considering part of the molecule close to the hydroxy group, HF ^{1}H isotropic chemical shifts of H2 and H4 are in good agreement with experiment (maximum difference 0.1 ppm), whereas DFT still gives a poorer description (maximum difference 0.23 ppm). With regard to carbon atoms HF always underestimates the C3 chemical shift (error ca. 3 ppm), whereas it correctly describes C2 and C4. On the other hand, DFT is precise for C3 and overestimates C2 and C4 isotropic chemical shifts (error ca. 2 ppm). However, the correlation coefficient R calculated for the whole molecule is better for hydrogen atoms when one calculates average values of chemical shifts ($R(HF)=0.994$ and $R(DFT)=0.987$), whereas this coefficient remains unchanged compared with separate rotamers for ^{13}C chemical shifts (see Table 1). In every case, the slope calculated by linear regression (theory versus experiment) is close to the ideal value of 1 and the intercept is close to zero. However,

the DFT intercept calculated for ^{13}C chemical shifts exhibits a large value (4 ppm) that can be interpreted as a systematic error due to the method. In order to make a final choice between the two computational strategies, root mean square difference (RMSD) and maximum errors were calculated. The results presented in Table 2 indicate that both theoretical strategies reproduce experimental isotropic chemical shifts with almost the same degree of accuracy (RMSD of less than 0.2 and 3 ppm for ^{1}H and ^{13}C, respectively). These deviations are essentially identical to those obtained for different molecular systems using different theoretical approach.[32,39–41] Consequently, we are confident about our calculations and we can conclude that HF calculation of isotropic chemical shifts with the 6-31G(d,p) basis set on HF/STO3-G-optimized geometry is a good alternative for reproducing the experimental NMR spectrum of cholesterol with sufficient accuracy.

Table 2. Root mean square difference (RMSD, in ppm), maximum theoretical error (max error, in ppm) compared with experiment, Pearson correlation coefficient *R*, slope and intercept (in ppm) of the least-squares regression line (theory versus experiment) for cholesterol and ergosterol with the two computational schemes (see text for details). All carbon or hydrogen atoms were used for the regression determination. Values in parenthesis correspond to the atom number for which the maximum error is observed.

	HF		DFT	
cholesterol	^{1}H	^{13}C	^{1}H	^{13}C
R	0.9936	0.9981	0.9873	0.9994
slope	1.05	0.96	0.98	0.96
intercept	−0.05	0.86	0.08	4.08
RMSD	0.13	2.36	0.16	2.68
max error	0.37 (6)	5.02 (14)	0.48 (15a)	5.48 (10)
ergosterol	^{1}H	^{13}C	^{1}H	^{13}C
R	0.9952	0.9985	0.9932	0.9995
slope	1.04	0.97	0.99	0.95
intercept	−0.04	1.24	0.06	4.56
RMSD	0.14	2.47	0.15	2.95
max error	0.29 (18)	5.02 (17)	0.29 (15a)	5.55 (10)

To confirm this strategy, the same analysis was performed on ergosterol. Its geometry was optimized and its ^{1}H and ^{13}C isotropic chemical shifts determined by using the previously proposed computational schemes. Calculations were compared with the experimental NMR spectrum of pure ergosterol in chloroform solution (this work and ref. [38]). The results presented in Tables 2 and 3 clearly indicate that the same degree of accuracy is achieved with both computational strategies. Moreover, we were able to reproduce the similar behavior of ^{1}H chemical shifts of the hydrogen atom close to the hydroxy group as a function of OH rotamer. This analogous behavior confirms the necessity of taking into account the average value of isotropic chemical shifts among the *anti*, *gauche*(−) and *gauche*(+) conformational isomers to simulate experimental NMR spectra of sterols in solution. Second, calculations on ergosterol confirm our previous conclusion that HF calculations with a medium-size basis set for spectroscopic calculations are sufficient to reach a good level of accuracy.

In calculations on both sterol molecules, statistical correlation (*R* value) is worse for ^{1}H chemical shifts than for ^{13}C chemical shifts with both theoretical approaches. This may be interpreted by the fact that the ^{1}H shielding constant is more sensitive than the ^{13}C shielding constant to the variation of C–H bond length.[42] The fact that geometry optimization with a minimal basis set (STO-3G) is adequate for this type of theoretical work is certainly related to the ring structure of sterols, which is a basic hydrocarbon skeleton without lone pairs and significant ionicity variations. Furthermore, molecular conformations are averaged in solution at room temperature, and thus, for comparison with experimental NMR data, low-level theoretical geometries appeared to be a good compromise between precision and computational time.

Despite the fact that we were able to find a reasonable computational strategy to calculate isotropic chemical shifts of two sterols, this study has revealed a peculiar behavior that is connected to the conformational rotameric states of the hydroxy-hydrogen atom. To elucidate this behavior, theoretical isotropic chemical shift differences between separate isomers and values calculated by averaging the contribution of each isomer were calculated. Results are reported in Figure 2 for both sterols at the HF level. Changes in the

Table 3. Ergosterol ^{13}C and ^{1}H theoretical chemical shift variations compared with experiment, $\delta_{theo}-\delta_{exp}$ (in ppm), calculated for atoms in positions 2–4.[a]

Position	Hartree–Fock							
	gauche(+)		*gauche*(−)		*anti*		Mean	
	^{13}C	^{1}H	^{13}C	^{1}H	^{13}C	^{1}H	^{13}C	^{1}H
2 (a)	1.24	0.30	1.11	−0.26	−1.57	0.26	0.26	0.10
2 (e)		−0.36		0.22		0.19		0.02
3	−2.42	0.08	−2.34	0.20	−2.39	0.07	−2.38	0.12
4 (a)	−2.15	0.19	0.68	−0.36	0.80	0.22	−0.22	0.02
4 (e)		0.10		0.16		−0.42		−0.05
R	0.9984	0.9913	0.9985	0.9919	0.9984	0.9907	0.9985	0.9952
Position	Density functional theory							
	gauche(+)		*gauche*(−)		*anti*		Mean	
	^{13}C	^{1}H	^{13}C	^{1}H	^{13}C	^{1}H	^{13}C	^{1}H
2 (a)	3.57	0.08	3.43	−0.38	−0.19	0.04	2.27	−0.09
2 (e)		−0.43		0.05		0.00		−0.12
3	−0.15	0.18	−0.10	0.01	−0.19	0.17	−0.15	0.12
4 (a)	0.02	0.10	4.00	−0.31	4.15	0.16	2.72	−0.01
4 (e)		−0.14		−0.04		−0.55		−0.24
R	0.9994	0.9909	0.9995	0.9908	0.9993	0.9896	0.9995	0.9932

[a] Chemical shifts were calculated with HF and DFT strategies (see text for details) for the three rotamers of ergosterol. The Pearson correlation coefficient *R* of the least-squares regression line (theory versus experiment) was calculated for all carbon or hydrogen atoms. Experimental chemical shifts were determined in chloroform solution as indicated in the Experimental Sction. Better *R* values are obtained by using mean values, both in the case of ^{13}C and ^{1}H. (a) and (e) denote axial and equatorial protons respectively.

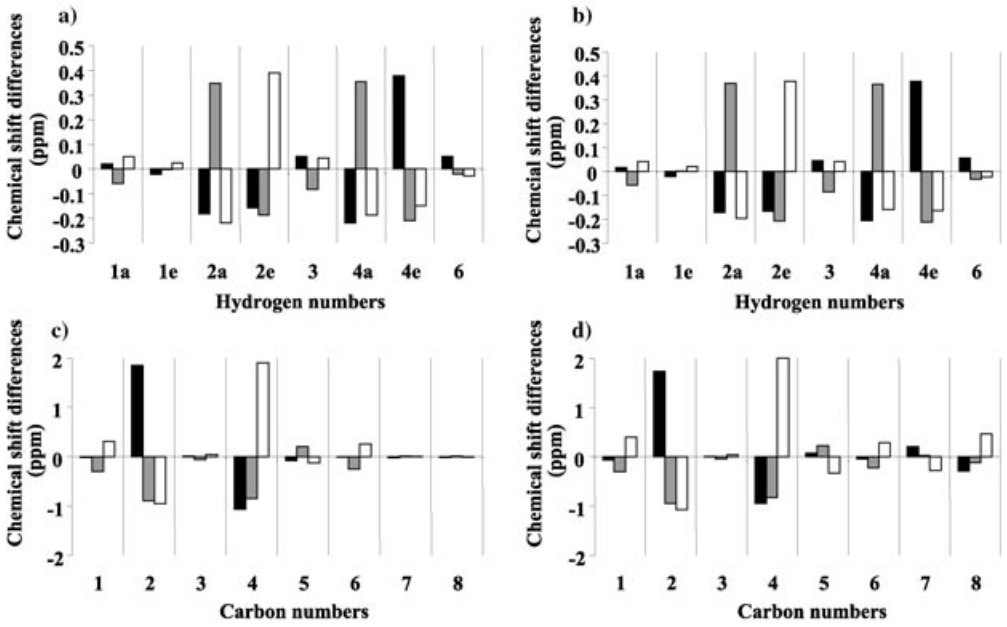

Figure 2. Theoretical isotropic chemical shift differences (in ppm) between separate isomers and values calculated by averaging the contribution of each isomer. a) ^{1}H chemical shifts of cholesterol. b) ^{1}H chemical shifts of ergosterol. c) ^{13}C chemical shifts of cholesterol. d) ^{13}C chemical shifts of ergosterol. Black, gray, and white bars correspond to *anti*, *gauche*(−) and *gauche*(+) isomers, respectively. Positions 9–19 show no significant differences and are not presented in the graphs. a: axial proton, e: equatorial proton.

conformation of the hydroxy-hydrogen atom leads to important modification of ^{1}H and ^{13}C NMR spectral patterns as compared with conformationally averaged spectra. For cholesterol, these variations affect atoms 1 to 6 both for ^{1}H and ^{13}C chemical shifts. For ergosterol, these deviations extend to atom 8. It is noteworthy that the largest varistions always involve atoms 2 and 4, as already mentioned above. Finally, while the details of the modifications are different, chemical shift variations still remain located on the same atoms at the DFT level (data not shown).

Hydrogen-bond effects on ^{13}C isotropic chemical shifts of cholesterol: To obtain more insight into variations in chemical shift induced by specific intermolecular interactions between cholesterol and different chemical groups that are present in the membrane environment, we performed several experimental and theoretical studies on two model systems. The first concerns modification of ^{13}C NMR spectra of cholesterol induced by the presence of acetone molecules that mimic carbonyl groups of membrane phospholipids. The second deals with the influence of water molecules that are present in the bulk membrane. A preliminary requirement is to demonstrate that our theoretical strategy is able to correctly describe specific intermolecular interactions and to reproduce ^{13}C isotropic chemical shift variations between pure cholesterol and cholesterol in the presence of acetone or water molecules, and possible other molecular partners.

Acetone–cholesterol interactions: We recorded NMR spectra of cholesterol in the presence of acetone (see Experimental Section). Chemical shift changes in cholesterol as a function of acetone/cholesterol molar ratio were determined for each atom and are presented in Figure 3 for C1 to C6. The first

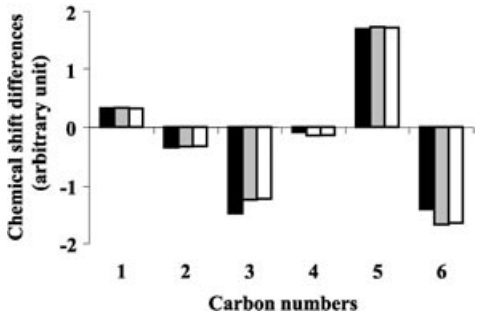

Figure 3. ^{13}C chemical shift variation (in ppm) between cholesterol associated with one acetone molecule and cholesterol in vacuum (theory) and in chloroform solution (experiment). Black bars: experiment; gray bars: theoretical cholesterol; white bars: theoretical two-ring model of cholesterol. The experimental data have been multiplied by the slope of the mean-squares regression line to conserve the same magnitude for chemical shift changes (see text for slope value).

observation is that the addition of acetone significantly affects only carbon atoms of rings A and B (atoms 1–6). The localization of these variations in a region close to the hydroxy group could be related to that observed for the ethanol–cholesterol interaction.[43] In this work, such modification has been interpreted in terms of hydrogen bonds between the cholesterol head group and ethanol molecules. Our experimental results can be interpreted in the same way, and theoretical quantum calculations of ^{13}C isotropic chemical shifts in the presence of acetone were performed to confirm this interpretation. Interaction between cholesterol and acetone must only be considered through the hydrogen atom of the cholesterol hydroxy group ($(CH_3)_2C{=}O_{acetone}\cdots H{-}O_{chol}$). Consequently, three structures were optimized corresponding to the three OH rotamers, each hydro-

gen-bonded to one acetone molecule. ^{13}C isotropic chemical shifts were calculated at the HF/6-31G(d,p) level on geometries fully optimized at the HF/STO-3G level according to our first computational strategy. The ^{13}C NMR spectrum of cholesterol in the presence of acetone was calculated by taking the average over the three rotamers, as already performed for pure cholesterol. Finally, the theoretical difference between cholesterol–acetone and pure cholesterol ^{13}C isotropic chemical shifts was calculated. It clearly appears that significant chemical shift variations are located on C1–6 (ring A), as already observed experimentally (values not shown). If one considers only chemical shift variations that occur on ring A, theoretical values qualitatively reproduce the experimental results (see Figure 3). For C1 and C5, the chemical shift difference is positive, whereas for the other four carbon atoms this difference is negative. The linear fit between theoretical and experimental values gives a Pearson coefficient of 0.9911 ($\delta_{theo}=247.30\,\delta_{exptl}-0.004$), and the RMSD is 0.15 ppm. This implies that our theoretical treatment of acetone–cholesterol interactions compared with pure cholesterol in solution reproduces with a good degree of accuracy the experimentally observed chemical shift modifications. The experimental data presented in Figure 3 have been multiplied by the slope of the mean square regression line in order to conserve the same magnitude for chemical shift changes. If one considers the theoretical treatment of the hydrogen bond, more accurate calculations can be envisaged by employing more flexible basis sets. However, it has been recently shown that STO-3G basis set is able to capture the solvent effects in the determination of NMR chemical shifts.[39]

A smaller molecular system was also used to demonstrate that one can reduce the computational effort for such study. Rings A and B were conserved in our molecular model of cholesterol, and C11 and C14 replaced by methyl groups. With this model, chemical shift differences between pure cholesterol and cholesterol interacting with acetone were determined with the above-mentioned procedure, and the results are displayed in Figure 3 together with the experimental data and calculations performed with the entire cholesterol molecule. The variations obtained with the small model of the cholesterol molecule are almost identical to those calculated by using the whole molecule. The Pearson coefficient of the linear fit between theoretical and experimental data is 0.9912 ($\delta_{theo}=244.39\,\delta_{exptl}-0.0005$), and the RMSD is 0.14 ppm. Therefore, the simulation of the whole molecular system (cholesterol + interacting molecule) is not necessary to reproduce physical effects that are located in the vicinity of the sterol hydroxy group. Consequently, the smaller molecular model will be used for further theoretical analysis of intermolecular interactions with cholesterol.

Water–cholesterol interactions: Among the different molecules and chemical groups that can interact with the polar region of cholesterol, water molecules constitute a highly probable candidate. Consequently, the influence of water–cholesterol interactions on ^{13}C chemical shifts of cholesterol was investigated in the same manner as for acetone. a solution of cholesterol in chloroform was titrated with water, and variation of ^{13}C chemical shifts was monitored as a function of water/cholesterol molar ratio. Again, the slope of the regression line (chemical shift variation as a function of water/cholesterol molar ratio) was determined for each carbon atom. Chemical shift variations compared with pure cholesterol are reported in Figure 4.

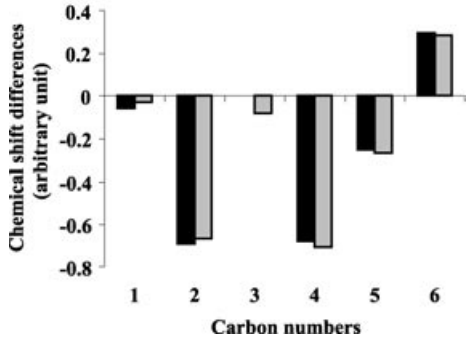

Figure 4. ^{13}C chemical shift variation (in ppm) between cholesterol associated with water molecules and cholesterol in vacuum (theory) and in chloroform solution (experiment). Black bars: experiment; gray bars: theoretical results with two-ring model. The experimental data have been multiplied by the slope of the mean-squares regression line to conserve the same magnitude for chemical shift changes (see text for slope value).

These variations are all negative except for C6 and have large amplitude for C2 and C4. This is different from those obtained with acetone and indicates that the nature of the hydrogen-bonding interactions must be different. Water can form hydrogen bonds to the cholesterol hydroxy group through its oxygen atom [$H_2O\cdots HO_{chol}$, denoted $H_2O(H)$] or through one of the two hydrogen atoms [$HOH\cdots OH_{chol}$, denoted $H_2O(O)$]. The two types of interaction were taken into account in the theoretical ^{13}C chemical shift calculations, and two situations were considered for $H_2O(O)$ hydrogen bonds, corresponding to interactions between water molecules and the two oxygen lone pairs. Variations relative to pure cholesterol were calculated by considering, for both cases, the average among the three rotamers. Results are displayed in Figure 5 for $H_2O(H)$ and $H_2O(O)$ hydrogen bonds together with results previously obtained with acetone for comparison. Chemical shift variations of cholesterol

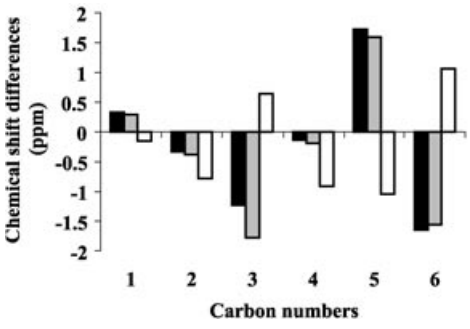

Figure 5. ^{13}C theoretical isotropic chemical shifts differences (in ppm) between cholesterol associated with one acetone molecule (black bars), one hydrogen-bond acceptor such as H_2O (gray bars), one hydrogen-bond donor such as H_2O (white bars) and cholesterol in vacuum.

are similar for hydrogen-bonding interaction to the hydroxy group through its hydrogen atom [either acetone or $H_2O(H)$].

In both cases, the variation is positive for C1 and C5, whereas it is negative for the four other carbon atoms. For $H_2O(O)$ hydrogen bonding, chemical shift variations are completely different. C1 and C5 exhibit a negative chemical shift difference, C3 and C6 a positive difference and C2 and C4 a larger negative difference. These results indicate that the variations in cholesterol chemical shifts depend on the nature of the hydrogen bond to the hydroxy group. The influence of a specific partner differs according to the site of attack, either the hydrogen or the oxygen atom of the hydroxy group. However, the chemical shift variations do not seem to be qualitatively affected by the nature of the partner that forms a hydrogen bond to a particular site. To reproduce the experimental chemical shift variations, one cannot consider only one specific hydrogen bond interaction. On the one hand, $H_2O(H)$ hydrogen bonding results in positive changes for C1 and C5. On the other hand, whereas $H_2O(O)$ hydrogen bonding leads to negative changes, the magnitude associated with C5 is too large compared to experimental data. Consequently, one must take into account both types of hydrogen bond to fit theoretical values to experimental one. Such a fit was obtained by adjusting the relative amounts of water involved in hydrogen bonding to the hydroxy H [$H_2O(H)$] and hydroxy O atoms [$H_2O(O)$] of cholesterol and averaging the chemical shifts of cholesterol over these different species. The best Pearson coefficient of the linear fit between theoretical and experimental data of 0.9981 ($\delta_{theo} = 130.79\,\delta_{exptl} + 0.052$) was obtained by using the following proportions: 30% of water in $H_2O(H)$ and 70% in $H_2O(O)$ hydrogen bonds. The best fit is shown in Figure 4, in which experimental data have been multiplied by the slope of the mean-squares regression line to conserve the same magnitude for chemical shift changes. These values reflect the possible hydrogen-bonding sites of the cholesterol hydroxy group. A maximum of one water molecule can form a hydrogen bond to the hydroxy hydrogen atom of cholesterol (H_{chol}), whereas the oxygen atom (O_{chol}) can be involved in hydrogen bonds with two water molecules interacting with the two oxygen lone pairs. Accordingly, the ratio between these two types of hydrogen bond is 1/3 for water hydrogen-bonded to H_{chol} and 2/3 for water hydrogen-bonded to O_{chol}, as approximately found by our best fit.

Conclusion

The aim of the work presented here was first to establish a quantum-chemical computational strategy that allows the accurate calculation of NMR isotropic chemical shifts of sterol-like molecular systems. We have shown that the HF level of theory with a minimal basis set (STO-3G) for geometry optimization and a medium-size basis set [6-31G(d,p)] for determination of chemical shifts is sufficient to achieve, with a low computational effort, accuracy as good as with the hybrid DFT approach. The comparison of theoretical chemical shifts with those experimentally obtained in chloroform unambiguously revealed that one must take the theoretical average values among three isoenergetic rotamers to reproduce ^1H and ^{13}C NMR spectra of cholesterol and ergosterol.

The second part of our work focused on the influence on cholesterol ^{13}C chemical shifts of specific molecules that may interact with cholesterol in a membrane. Titration experiments with acetone or water revealed variations in ^{13}C chemical shifts essentially located on the two first rings of cholesterol (C1–C6). To clarify the nature of specific interactions with cholesterol, quantum-chemical calculations were performed on the acetone– and water–cholesterol systems by only considering hydrogen bonds to the cholesterol hydroxy group 3β-OH. These calculations revealed the aptitude of our computational strategy to correctly take into account the effect of these specific interactions. We were able to reproduce the experimental variations in chemical shifts by using average values among the three rotamers and by using specific hydrogen-bond populations that are consistent with chemical intuition. This theoretical approach has also demonstrated the specific influence of hydrogen-bond type—either with the hydrogen or the oxygen atom of the sterol hydroxy group—on ^{13}C NMR spectra.

Thus, we have established a quantum-chemical computational strategy that allows both the accurate calculation of isotropic chemical shifts and of specific hydrogen-bond effects. This theoretical tool will be further used to understand the nature of specific molecular interactions in cholesterol–phospholipid systems highlighted by solid-state NMR experiments.

Experimental Section

NMR experiments: Cholesterol (≥99%, Aldrich) and ergosterol (≥90%, Aldrich) were desiccated overnight to eliminate residual water and dissolved in anhydrous $CDCl_3$ ($HDO + D_2O \leq 0.01\%$, Euriso-top) to 10 mM concentration. Dry acetone ($HDO + D_2O \leq 0.01\%$) and deuterium-depleted water used in titration experiments were purchased from Euriso-top and Aldrich, respectively.

The NMR experiments were performed on a Bruker DMX narrow-bore spectrometer operating at a ^1H Larmor frequency of 500.13 MHz equipped with a pulsed-field gradient double-resonance probe ($T = 295$ K). ^1H and ^{13}C assignments were obtained by recording 1D spectra (^{13}C spectra recorded with single π/2 pulse or INEPT polarization transfer) and 2D homonuclear or heteronuclear spectra (DQF-COSY, HMQC, HMBC) with typical Bruker pulse programs. All spectra were calibrated by using $CDCl_3$ resonances at 7.27 and 77 ppm for ^1H and ^{13}C, respectively. Typical π/2 pulses were 5 μs and 10 μs for ^1H and ^{13}C nuclei, respectively.

For titration experiments, ^{13}C 1D spectra were recorded for different acetone (or water)/cholesterol molar ratios in $CDCl_3$ solutions. The molar ratio was varied between 0 and 17 for acetone/cholesterol and 0 and 3 for water/cholesterol. Chemical shift changes of cholesterol were then monitored as a function of the molar ratio. For each cholesterol carbon atom, saturation effect was never observed, and slopes corresponding to the linear variation of chemical shifts with molar ratio were calculated. The slopes for C7–C16 were almost identical, and the average of these slopes was subtracted from all carbon data to obtain the specific variation due to hydrogen bonding.

Computational methods: The principal aim of this work was to calibrate a computational method that allows efficient and accurate calculations of NMR isotropic chemical shifts of sterols. To this end, theoretical ^{13}C and ^1H NMR isotropic chemical shifts δ_{iso} were compared with data obtained

experimentally on sterols in solution. Thus, we are meeting the crucial issue of molecular modeling, that is, obtaining the best theoretical values with the least computational effort. Consequently, two problems of different nature must be resolved. First, one must determine the optimum method for geometry optimizations. Second, the electronic-structure problem associated with NMR computations must be resolved with sufficient accuracy. For the latter, it is well known that theoretical chemical shieldings σ are highly sensitive to the choice of basis set.[30] The basis set must be sufficiently flexible to correctly describe the electron density of the molecular system but not too large in order to reduce the computational cost. Thus, we chose a double-zeta basis set augmented by polarization functions on all atoms, namely, the 6-31G(d,p) basis set,[44] for all NMR calculations. This basis set has been used in several theoretical works and has proven its suitability for reproducing NMR chemical shifts for large molecular systems.[45–49] We also investigated the choice of the quantum-chemical method by performing NMR calculations using the Hartree–Fock method and the hybrid DFT method B3LYP, which includes part of the electronic correlation.[35,36] In all cases, among the various theories available to calculate chemical shielding tensors, the Gauge Including Atomic Orbital (GIAO) method was adopted for the numerous advantages it offers.[50–54]

For geometry optimization, two strategies were tested: a computationally inexpensive one that combines the HF method with a minimal STO-3G basis set[44] and a more costly one that involves the B3LYP method and the 6-31G(d,p) basis set. If one then combines the structure and NMR problems, one obtains four computational schemes. However, we decided to investigate only two alternatives. First, NMR calculations were performed at the HF level on structures optimized at the HF level with the minimal STO-3G basis set (denoted HF/6-31G(d,p)//HF/STO-3G). Second, NMR calculations were performed with the B3LYP method and 6-31G(d,p) basis set on geometries optimised at the same level (denoted B3LYP6-31G(d,p)//B3LYP6-31G(d,p)). For the sake of simplicity, we will use HF and DFT to denote the two methods. All calculations were performed with the Gaussian 98 package.[55]

In the liquid state, the observable quantity is the isotropic chemical shift $\delta_{iso} = \sigma_{iso}^{ref} - \sigma_{iso}$ where σ_{iso} and σ_{iso}^{ref} are the isotropic chemical shieldings of the compound of interest and of the standard reference compound (tetramethylsilane, TMS), respectively. ^{13}C and ^{1}H NMR chemical shieldings of TMS were calculated with both computational strategies. Theoretical isotropic chemical shifts δ_{iso} of sterols were obtained by using values of isotropic chemical shieldings calculated at the same level of theory so that the same errors due to the method were introduced for both values of σ_{iso}. Theoretical ^{13}C and ^{1}H isotropic chemical shieldings of TMS used in this work are given in Table 4.

Table 4. Theoretical TMS ^{13}C and ^{1}H chemical shielding (in ppm) obtained by the two computational strategies. Computational details are given in the Experimental Section.

Atom	HF/6-31G(d,p)// HF-STO-3G	B3LYP6-31G(d,p)// B3LYP6-31G(d,p)
^{13}C	204.66	191.89
^{1}H	32.56	31.75

Concerning interactions of cholesterol with acetone or water, we used the supermolecule model to simulate specific hydrogen bonding to the hydroxy group of cholesterol (see below for more details of calculations). Note that this work aims to reproduce isotropic chemical shifts on systems in liquid phase. Ideally, one would do molecular dynamics averaging at finite temperature on sterol *n*-mers or on the sterol–acetone or sterol–water molecular system to obtain a reasonable representation of solution isotropic shifts. Moreover, this procedure would have the advantage of including a large number of possible molecular configurations in solution, whereby the shieldings are calculated for each configuration, weighted by a factor that depends on appropriate partition functions.[39,56–58] However, since the number of configurations in solution is huge, this type of theoretical approach remains computationally very expensive, and this goal is almost unachievable in an affordable time. Thus, optimization of geometries in vacuum, which is a standard procedure in quantum chemistry, is still reasonable. If one only uses the agreement between experimental and calculated NMR chemical shieldings as a criterion of success, it is conceivable that good agreement can be reached by the use of optimized geometries that underestimate the interatomic bond lengths in conjunction with a method of calculating chemical shifts that underestimates the shielding or vice versa.[32]

Finally, in the supermolecule approach using either small or medium-size basis sets, it is well known that calculations can be subject to basis set superposition errors (BSSE). Consequently, the counterpoise method[59] using ghost orbitals for the GIAO calculations was employed for the acetone–cholesterol and water–cholesterol molecular systems to estimate the error in the calculation of chemical shifts when BSSE is neglected (data not shown). For both molecular systems, the root mean square difference of ^{13}C chemical shifts with and without counterpoise ghost orbitals is about 0.07 ppm, which is a relatively small error compared with the chemical shifts variations that we intend to reproduce. These results are in agreement with previous theoretical works.[42,60,61]

Acknowledgement

This work was financed by a concerted action of the French Ministry of Research, CNRS and the University Paul Sabatier.

[1] P. L. Yeagle, *Biochim. Biophys. Acta* **1985**, *822*, 267.
[2] H. U. Gally, A. Seelig, J. Seelig, *Hoppe-Seyler's Z. Physiol. Chem.* **1976**, *357*, 1447.
[3] G. W. Stockton, I. C. Smith, *Chem. Phys. Lipids* **1976**, *17*, 251.
[4] D. Chapman, N. F. Owens, M. C. Phillips, D. A. Walker, *Biochim. Biophys. Acta* **1969**, *183*, 458.
[5] J. M. Smaby, H. L. Brockman, R. E. Brown, *Biochemistry* **1994**, *33*, 9135.
[6] G. Smutzer, P. L. Yeagle, *Biochim. Biophys. Acta* **1985**, *814*, 274.
[7] M. Straume, B. J. Litman, *Biochemistry* **1987**, *26*, 5121.
[8] T. P. W. McMullen, R. N. McElhaney, *Curr. Opin. Colloid Interface Sci.* **1996**, *1*, 83.
[9] H. Ohvo-Rekila, B. Ramstedt, P. Leppimaki, J. P. Slotte, *Prog. Lipid Res.* **2002**, *41*, 66.
[10] M. P. Marsan, I. Muller, C. Ramos, F. Rodriguez, E. J. Dufourc, J. Czaplicki, A. Milon, *Biophys. J.* **1999**, *76*, 351.
[11] C. Gliss, O. Randel, H. Casalta, E. Sackmann, R. Zorn, T. Bayerl, *Biophys. J.* **1999**, *77*, 331.
[12] R. Bittman, *Cholesterol: Its Function and Metabolism in Biology and Medicine*, Plenum Press, New York, **1997**, p. 145.
[13] P. L. Yeagle in *Biology of Cholesterol*, (Ed.: P. L. Yeagle), Academic Publishers, Boca Raton, **1988**, p. 121.
[14] J. H. Davis in *Cholesterol in Membrane Models*, (Ed.: L. Finegold), CRC Press, Boca Raton, **1993**, p. 67.
[15] E. J. Dufourc, E. J. Parish, S. Chitrakorn, I. C. P. Smith, *Biochemistry* **1984**, *23*, 6062.
[16] D. L. Worcester, N. P. Franks, *J. Mol. Biol.* **1976**, *100*, 359.
[17] J. N. Israelachvili, *Intermolecular and Surface Forces: with Application to Colloidal and Biological Systems*, Academic Press, London, **1989**.
[18] T. P. McMullen, R. N. Lewis, R. N. McElhaney, *Biochemistry* **1993**, *32*, 516.
[19] J. P. Slotte, *Chem. Phys. Lipids* **1999**, *102*, 13.
[20] M. B. Sankaram, T. E. Thompson, *Biochemistry* **1990**, *29*, 10676.
[21] J. M. Boggs, *Biochim. Biophys. Acta* **1987**, *906*, 353.
[22] F. T. Presti, R. J. Pace, S. I. Chan, *Biochemistry* **1982**, *21*, 3831.
[23] R. Bittman, C. R. Kasireddy, P. Mattjus, J. P. Slotte, *Biochemistry* **1994**, *33*, 11776.
[24] H. L. Scott, *Biophys. J.* **1991**, *59*, 445.
[25] M. Pasenkiewicz-Gierula, Y. Takaoka, H. Miyagawa, K. Kitamura, A. Kusumi, *J. Phys. Chem. A* **1997**, *101*, 3677.
[26] K. Tu, M. L. Klein, D. J. Tobias, *Biophys. J.* **1998**, *75*, 2147.
[27] A. M. Smondyrev, M. L. Berkowitz, *Biophys. J.* **1999**, *77*, 2075.

[28] T. J. O'Leary in *Cholesterol in Membrane Models*, (Ed.: L. Finegold), CRC Press, Boca Raton, **1993**, p. 175.
[29] T. Helgaker, M. Jaszunski, K. Ruud, *Chem. Rev.* **1999**, *99*, 293.
[30] A. C. de Dios, *Prog. Nucl. Magn. Reson. Spectrosc.* **1996**, *29*, 229.
[31] A. C. de Dios, E. Oldfield, *Solid State Nucl. Magn. Reson.* **1996**, *6*, 101.
[32] J. C. Facelli, *Concepts Magn. Reson. Part A* **2004**, *20*, 42.
[33] E. Virtanen, M. Nissinen, R. Suontamo, J. Tamminen, E. Kolehmainen, *J. Mol. Struct.* **2003**, *649*, 207.
[34] E. Virtanen, A. Valkonen, J. Tamminen, E. Kolehmainen, *J. Mol. Struct.* **2003**, *650*, 201.
[35] A. D. J. Becke, *J. Chem. Phys.* **1993**, *98*, 5648.
[36] C. Lee, W. Yang, R. G. Parr, *Phys. Rev. B* **1988**, *37*, 785.
[37] H.-S. Shieh, L. G. Hoard, C. E. Nordman, *Acta Crystallogr.* **1981**, *37*, 1538.
[38] W. K. Wilson, R. M. Sumpter, J. J. Warren, P. S. Rogers, B. Ruan, G. J. Schroepfer, Jr., *J. Lipid Res.* **1996**, *37*, 1529.
[39] J. Casanovas, A. M. Namba, S. Leon, G. L. Aquino, G. V. da Silva, C. Aleman, *J. Org. Chem.* **2001**, *66*, 3775.
[40] S. Saen-oon, S. Hannongbua, P. Wolschann, *J. Chem. Inf. Comput. Sci.* **2003**, *43*, 1412.
[41] M. Strohmeier, D. M. Grant, *J. Am. Chem. Soc.* **2004**, *126*, 966.
[42] M. Pecul, K. Jackowski, K. Wozniak, J. Sadej, *Solid State Nucl. Magn. Reson.* **1997**, *8*, 138.
[43] V. A. Daragan, A. M. Voloshin, S. V. Chochina, T. N. Khazanovich, W. G. Wood, N. A. Avdulov, K. H. Mayo, *Biophys. J.* **2000**, *79*, 406.
[44] Description of basis sets can be found in A. E. Foresman in *Exploring Chemistry with Electronic Structure Methods*, 2nd ed., Gaussian Inc., Pittsburgh, **1998**.
[45] G. Sun, M. Kertesz, *J. Phys. Chem. A* **2001**, *105*, 5468.
[46] J. R. Cheeseman, G. W. Trucks, T. A. Keith, M. J. J. Frisch, *J. Chem. Phys.* **1996**, *104*, 5497.
[47] P. B. Karadakov, *J. Mol. Struct.* **2002**, *602*, 293.
[48] G. Barone, D. Duca, A. Silvestri, L. Gomez-Paloma, R. Riccio, G. Bifulco, *Chem. Eur. J.* **2002**, *8*, 3240.
[49] L. Pejov, D. Vikic-Topic, *J. Chem. Inf. Comput. Sci.* **2001**, *41*, 1478.
[50] K. Wolinski, J. F. Hilton, P. Pulay, *J. Am. Chem. Soc.* **1990**, *112*, 8251.
[51] J. L. Dodds, R. McWeeny, A. J. Sadlej, *Mol. Phys.* **1980**, *41*, 1419.
[52] R. Ditchfield, *Mol. Phys.* **1974**, *27*, 789.
[53] R. McWeeny, *Phys. Rev.* **1962**, *126*, 1028.
[54] F. J. London, *J. Phys. Radium* **1937**, *8*, 397.
[55] Gaussian 98, Revision A9, M. J. Frisch, G. W. Trucks, H. B. Schlegel, G. E. Scuseria, M. A. Robb, J. R. Cheeseman, V. G. Zakrzewski, J. A. Montgomery, R. E. Stratmann, Jr., J. C. Burant, S. Dapprich, J. M. Millam, A. D. Daniels, K. N. Kudin, M. C. Strain, O. Farkas, J. Tomasi, V. Barone, M. Cossi, R. Cammi, B. Mennucci, C. Pomelli, C. Adamo, S. Clifford, J. Ochterski, G. A. Petersson, P. Y. Ayala, Q. Cui, K. Morokuma, D. K. Malick, A. D. Rabuck, K. Raghavachari, J. B. Foresman, J. V. Ortiz, J. Cioslowski, B. B. Stefanov, G. Liu, A. Liashenko, P. Piskorz, I. Komaromi, R. Gomperts, R. L. Martin, D. J. Fox, T. Keith, M. A. Al-Laham, C. Y. Peng, A. Nanayakkara, C. Gonzalez, M. Challacombe, P. M. W. Gill, B. Johnson, W. Chen, M. W. Wong, J. L. Andres, C. Gonzalez, M. Head-Gordon, E. S. Replogle, J. A. Pople, Gaussian, Inc., Pittsburgh, PA, **1998**.
[56] R. Ludwig, F. Weinhold, T. C. Farrar, *J. Phys. Chem. A* **1997**, *101*, 8861.
[57] R. Ludwig, F. Weinhold, T. C. Farrar, *J. Chem. Phys.* **1997**, *107*, 499.
[58] J. Ropp, C. Lawrence, T. C. Farrar, J. L. Skinner, *J. Am. Chem. Soc.* **2001**, *123*, 8047.
[59] S. F. Boys, F. Bernardi, *Mol. Phys.* **1970**, *19*, 553.
[60] S. Ferchiou, C. Giessner-Prette, *Chem. Phys. Lett.* **1983**, *103*, 156.
[61] K. Jackowski, E. Wielogorska, *J. Mol. Struct.* **1995**, *355*, 287.

Received: March 15, 2004
Revised: July 13, 2004
Published online: October 21, 2004

